
Shear-induced turbulent mixing in stratocumulus layer

JEANNINE KATZWINKEL * AND HOLGER SIEBERT

Leibniz Institut for Tropospheric Research, Leipzig, Germany

RAYMOND A. SHAW

Michigan Technological University Houghton, Michigan, USA

1. Introduction

Stratiform clouds are widespread and play an important role in the Earth's radiation and energy balance. In particular the microphysical structure of the cloud top is most important: on the one hand, most of the incoming shortwave radiation is affected by the cloud in the first couple of ten meters, and on the other hand this region is highly influenced by the entrainment process through which dry (sub-saturated) and potentially warmer air is mixed into the cloud from above. The classical picture of the entrainment process is based on cloudy air parcels which become negatively buoyant due to partially radiative cooling at cloud top. These descending cloud parcels drive the mixing process. However, large-scale wind shear also can induce turbulence with subsequent mixing.

The investigation of the detailed turbulent entrainment process benefits from high-resolution measurements, which are difficult to obtain with fast-flying research aircraft. Therefore, the helicopter-borne measurement payload "ACTOS" (Airborne Cloud Turbulence Observation System) was used to investigate the top of a stratiform cloud layer with high spatial and temporal resolution. This paper deals with the in-situ observation of one particular case in which wind shear was observed to be important. Specifically, the shear resulted in a turbulent but drop-free sublayer inside the lower part of the temperature inversion above the cloud top.

2. Experiments

ACTOS is a helicopter-borne measurement payload designed for high-resolution measurements of turbulence and other cloud parameters in atmospheric boundary-layer clouds. A detailed description of the payload is given in Siebert et al. (2006a). The three dimensional wind vector is measured with an ultrasonic anemometer of type Solent HS with a frequency of 100 Hz. The temperature is detected with an Ultra-Fast Thermometer and a Particle Volume Monitor (PVM-100A) measures the liquid water content (LWC). ACTOS is attached to the helicopter by a 140 m long rope, which assures stable flight conditions and a negligible influence of the rotor downwash. The helicopter

operates at a true air speed (TAS) of $15 - 20 \text{ m s}^{-1}$.

The measurements were performed in and above a stratocumulus layer over the Baltic Sea in October 2007. During one flight several gradual ascents and descents were performed, in which the payload was dipped into the cloud from above while the helicopter remained outside (so-called "Dolphin flights"). Hence, data are collected inside the cloud layer, the inversion layer with the turbulent sublayer, and inside the lower free atmosphere.

3. Results and discussion

The flight of October 8, 2007 consists of six profiles beginning inside the cloud layer up to the lower free atmosphere, and back down again. On average, the cloud region is characterized by a mean LWC of 0.3 g m^{-3} , an absolute humidity of 5 g m^{-3} and a temperature of 1°C . The lower free atmosphere indicates an absolute humidity of 0.1 g m^{-3} and the temperature increases to 7°C . The number of interstitial aerosol decreases from 700 cm^{-3} inside the cloud layer to around 150 cm^{-3} in the free atmosphere. As an example, the data from one profile are shown in Fig. 1.

The cloud top (simply defined by the absence of cloud droplets) is located at 1289 m for the descent shown in Fig. 1. Above cloud top is a clearly defined layer with increasing potential temperature, the temperature inversion denoted by the two green lines in Fig. 1. The inversion layer can be distinguished by two sublayers: i) the lower part, which we call the "turbulent sublayer," seems to be an "old cloud layer" where the cloud droplets are evaporated, resulting in a local increase of the interstitial aerosol concentration N around cloud top, followed by ii) the much less turbulent "residual inversion layer."

The turbulent layer is also characterized by a strong wind shear which is likely to enhance the entrainment and the mixing process between the moist, but unsaturated air of the sublayer with cloudy air. The increased turbulent mixing in that region is documented by the high values of the variance of the vertical wind velocity. Furthermore, the

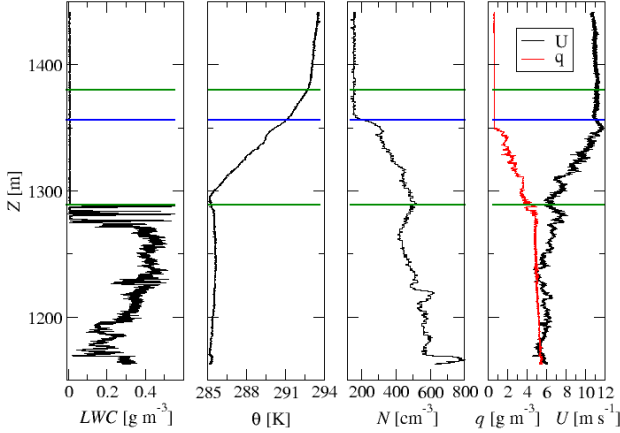


FIG. 1. Profiles of liquid water content (LWC), potential temperature (Θ), number of interstitial aerosol (N) and absolute humidity (q) over a single descent. The temperature inversion lies between the two green lines — the top of the turbulent sublayer is marked with a blue line.

gradient Richardson number

$$Ri = \frac{g}{\Theta} \frac{\frac{\partial \bar{\Theta}}{\partial z}}{\left(\frac{\partial \bar{U}}{\partial z}\right)^2}$$

is still below the critical value which allows turbulence to develop (see Fig. 2).

The local energy dissipation rate ε (derived from second-order structure functions of 1-s-long subrecords, see Siebert et al. (2006b) for more details) does not significantly vary between the cloud layer and the turbulent sublayer. This indicates that the cloud layer and turbulent sublayer are strongly coupled through turbulent mixing. Maximum values of above $10^{-2} \text{m}^2 \text{s}^{-3}$ are found in the turbulent sublayer which indicates comparably strong turbulence. Inside the “residual inversion layer” ε decreases suddenly to values of about $10^{-4} \text{m}^2 \text{s}^{-3}$, indicating weak turbulence. The residual inversion layer is characterized by almost no shear, a gradient Richardson number much higher than one and all turbulence parameters represent similar properties as inside the free atmosphere.

A turbulent sublayer was detected in all six profiles of the measurement flight. The descent represented above has a sublayer thickness of 67 m, but for all profiles it varies between 37 m and 85.5 m indicating either some spatial variability of the entrainment process or might the different stages of the sublayer evolution. The thickness of the residual inversion layer always decreases with increasing sublayer thickness, until, in two cases, the turbulent sublayer takes up the whole temperature inversion layer.

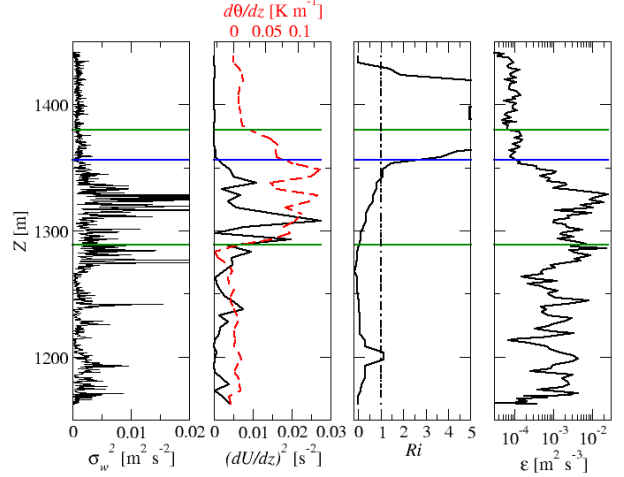


FIG. 2. Profiles of variance of the vertical wind component σ_w^2 , wind shear ($(dU/dz)^2$), temperature gradient ($d\Theta/dz$), gradient Richardson number (Ri) and energy dissipation rate (ε). The temperature inversion is located between the green lines and the lower part represents the turbulent sublayer.

The varying thickness of the turbulent sublayers has consequences for parameters such as the wind shear, Richardson number, and local turbulent energy dissipation rate within the turbulent sublayer. Furthermore, it seems also to influence the LWC at cloud top. Figure 3 shows the mean wind shear, temperature gradient, Richardson number and the LWC at cloud top as a function of the thickness of the turbulent sublayer.

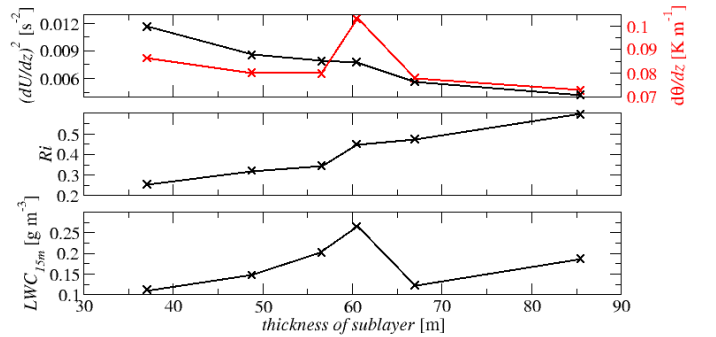


FIG. 3. Influence of the sublayer thickness on the stability, shear, gradient Richardson number and the mean liquid water content of the upper 15 m of the cloud.

Due to increasing thickness of the turbulent layer all gradients are consequently decreasing. However, this decrease is in such a way that the Richardson number (al-

though slightly increasing) is still below the critical value so that the wind shear is strong enough and turbulence can persist in this region.

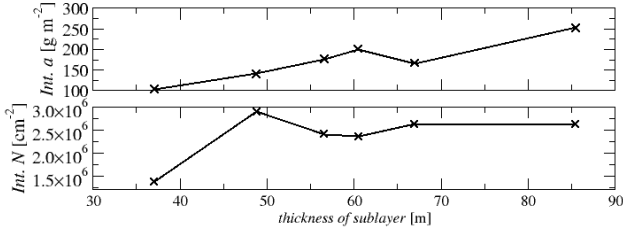


FIG. 4. Influence of the sublayer thickness on the absolute values of the absolute humidity ($Int. a$) and the number of interstitial aerosol ($Int. N$) integrated over the turbulent sublayer.

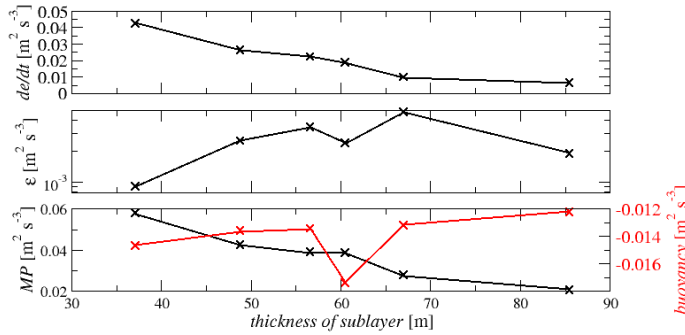


FIG. 5. Influence of the sublayer thickness on the temporal derivation of the kinetic energy, energy dissipation rate, shear part and buoyancy part.

The wind shear inside the thin sublayer leads to the mixing process of mostly moist sublayer air (and maybe partly dry air from the residual inversion) with cloudy air, followed by the evaporation of cloud droplets. Consequently, additional aerosol remains inside the sublayer evident on the absolute number of aerosol integrated over the turbulent sublayer, presented in Fig. 5. Additionally, the absolute values of the absolute humidity, also integrated over the turbulent sublayer, indicates further moistening of the sublayer region (Fig. 5). The constance of both parameter at the bottom of the sublayer support a continuously mixing between sublayer and cloudy air. At the top of the sublayer both parameter decreases with sublayer thickness indicating an increase mixing of the residual inversion layer and the sublayer top with growing sublayer. Nevertheless, the sublayer grows of the expense of the residual inversion layer and the cloud layer. Since the air entrained into the cloud top becomes more and more moist, a decrease of the evaporation rate of the droplets can be expected. Consequently, the LWC of the upper 15 m of the cloud is less

reduced due to evaporation with increasing sublayer thickness.

The mechanical production of turbulent kinetic energy due to shear decreases with increasing sublayer thickness whereas the buoyancy contribution seems to be independent of the sublayer thickness (see Fig. 5). Hence, the balance of the temporal derivation of the turbulent kinetic energy decreases with increasing sublayer thickness. The energy dissipation rate (averaged over the turbulent sublayer) seems also to be independent of the thickness of the sublayer. The two values at a sublayer thickness of 85.5 m and 60.2 m belong to the two cases in which the sublayer takes up the whole temperature inversion layer.

Similar observations of such turbulent sublayers above cloud tops have been made in a few numerical simulations. Moeng et al. (2005) simulated this bisection of the temperature inversion layer and pointed out that the sublayer is always present, fully turbulent, but unsaturated. The “residual inversion layer” above, is unsaturated and non-turbulent except maybe intermittent turbulence due to local shear events. The LES simulations of Wang et al. (2008) result in a close connection between the sublayer thickness and the mean wind shear across the inversion layer which is in agreement to our observations and the observations of Wang (2010). Related observations in real atmospheric clouds were made by Rogers and Telford (1986), who also found a thin subsaturated but turbulent layer above cloud top. The variability of the turbulent sublayer is observed by Wang (2006).

REFERENCES

- CH Moeng, B. Stevens, and PP Sullivan. Where is the Interface of the Stratocumulus-Topped PBL? *Journal of the Atmospheric Sciences*, 62(7):2626–2631, 2005.
- D. P. Rogers and J. W. Telford. Metastable stratus tops. 112:481–500, 1986.
- H. Siebert, H. Franke, K. Lehmann, R. Maser, E. W. Saw, D. Schell, R. A. Shaw, and M. Wendisch. Probing fine-scale dynamics and microphysics of clouds with helicopter-borne measurements. 87:1727 – 1738, 2006a.
- H. Siebert, K. Lehmann, and M. Wendisch. Observations of small scale turbulence and energy dissipation rates in the cloudy boundary layer. 63:1451 – 1466, 2006b.
- Q. Wang. Entrainment and the fine structure of the stratocumulus cloud top. In *17th Symposium on Boundary Layers and Turbulence*, 2006.
- Q. Wang. Wind shear and thermodynamic characteristics near the stratocumulus cloud top. In *13th Conference on Cloud Physics*, 2010.

S. Wang, J.C. Golaz, and Q. Wang. Effect of intense wind shear across the inversion on stratocumulus clouds. *Geophysical Research Letters*, 35:L15814, 2008.